Human-observer LROC study of lesion detection in Ga-67 SPECT images reconstructed using MAP with anatomical priors

Andre Lehovich, *Member, IEEE,* Philippe P. Bruyant, Howard C. Gifford, *Member, IEEE,* Peter B. Schneider, Shane Squires, Robert Licho, Gene Gindi, *Member, IEEE,* and Michael A. King, *Senior Member, IEEE*

***Abstract*— We compare the image quality of SPECT reconstruction with and without an anatomical prior. Area under the localization-response operating characteristic (LROC) curve is our figure of merit. Simulated Ga-67 citrate images, a SPECT lymphnodule imaging agent, were generated using the MCAT digital phantom. Reconstructed images were read by human observers.**

Several reconstruction strategies are compared, including rescaled block iterative (RBI) and maximum-a-posteriori (MAP) with various priors. We find that MAP reconstruction using prior knowledge of organ and lesion boundaries significantly improves lesion-detection performance ($p < 0.05$). Pseudo-lesion boundaries, regions without increased uptake which are incorrectly treated as prior knowledge of lesion boundaries, do not decrease performance.

***Index Terms*— SPECT reconstruction, anatomical priors, LROC, human observer study**

I. Introduction

DUAL-MODALITY systems capable of providing physically registered images from x-ray computed tomography (CT) and single-photon emission computed tomography (SPECT) are beginning to have widespread clinical use. In previous work we have presented evidence suggesting it may be possible to improve SPECT image quality by providing the SPECT reconstruction algorithm with anatomical information, for example the boundaries of organs or lesions gleaned from CT data [1]–[3].

This paper expands on those results by having human observers, including nuclear-medicine physicians, perform a lesion search task on images reconstructed from simulated SPECT data. We compute localization-response operating characteristic (LROC) curves and use area under the curve (AUC) as the figure of merit to compare reconstruction algorithms. A total of nine algorithms are evaluated, including rescaled block iterative (RBI), and a variety of maximum a-posteriori (MAP) approaches incorporating varying amounts of prior knowledge about the anatomy.

Prior anatomical knowledge may consist of organ boundaries or lesion boundaries. Using the boundaries of "pseudo lesions", small structures visible in CT but which do not have increased radiotracer uptake, might induce false positives due to noise correlation [4]. One example a pseudo-lesion is a necrotic tumor which is visible in CT but not in SPECT. To assess this effect, we also include pseudo lesions in some of our anatomical priors.

Manuscript received 17 November, 2006. This work was supported by the National Institute of Biomedical Imaging and Bioengineering under grant number R01-EB02798. The contents are solely the responsibility of the authors and do not necessarily represent the views of the granting agency.

A. Lehovich, H. C. Gifford, P. B. Schneider, S. Squires, R. Licho, and M. A. King are with the Division of Nuclear Medicine, Department of Radiology, University of Massachusetts Medical School, 55 Lake Ave N., Worcester, MA 01655 USA (email: Andre.Lehovich@umassmed.edu).

P. P. Bruyant is with the Université de Bretagne Occidentale, 5 Avenue Foch 29609 Brest, France.

G. Gindi is with the Department of Radiology, State University of New York, Stony Brook, NY 11794-8460 USA.

II. Methods

A. Data generation

Gallium citrate is a SPECT lymphoma imaging agent [5], [6]. The Mathematical Cardiac Torso (MCAT) digital phantom was used to create $128 \times 128 \times 128$ voxel maps of the distribution of ^{67}Ga citrate and attenuation in the chest [7], [8]. 1-cm spherical lesions at various locations were added to the MCAT background. Simulated projection images were then generated from the MCAT maps using the SIMIND Monte Carlo package [9].

B. Image reconstruction

Each simulated data set produced by SIMIND was reconstructed using nine reconstruction strategies. As a baseline we used the rescaled block-iterative (RBI) algorithm which had been optimized by previous model- and human-observer studies [10], [11]. We also included two MAP strategies using simple quadratic smoothing with no anatomical prior, differing only in the strength of the smoothing prior.

The parameter β controls the amount of smoothing; higher values give more smoothing. Two values, $\beta = 0.005$ and $\beta = 0.04$ were chosen based on a preliminary study using model observers.

We also used MAP reconstruction with three types of anatomical priors: organ boundaries, organ boundaries plus lesion boundaries only when the lesion was present, and organ boundaries plus lesion boundaries when the lesion was present plus pseudo-lesion boundaries when the lesion was absent. Quadratic smoothing using a 3-D neighborhood was performed within each anatomical region, but not across anatomical

1-4244-0561-0/06/$20.00 ©2006 IEEE.

TABLE I

RECONSTRUCTION STRATEGIES UNDER COMPARISON.

code	description
RBI	RBI, no prior, $\beta = 0.0$
w	MAP, weak quadratic prior, $\beta = 0.005$
s	MAP, stronger quadratic prior, $\beta = 0.04$
wO	MAP, weak anatomical prior using organ boundaries, $\beta = 0.005$
sO	MAP, stronger anatomical prior using organ boundaries, $\beta = 0.04$
wO+L	MAP, weak anatomical prior using organ and true-lesion boundaries, $\beta = 0.005$
sO+L	MAP, stronger anatomical prior using organ and true-lesion boundaries, $\beta = 0.04$
wO+P	MAP, weak anatomical prior using organ, true lesion, and pseudo-lesion boundaries, $\beta = 0.005$
sO+P	MAP, stronger anatomical prior using organ, true-lesion and pseudo-lesion boundaries, $\beta = 0.04$

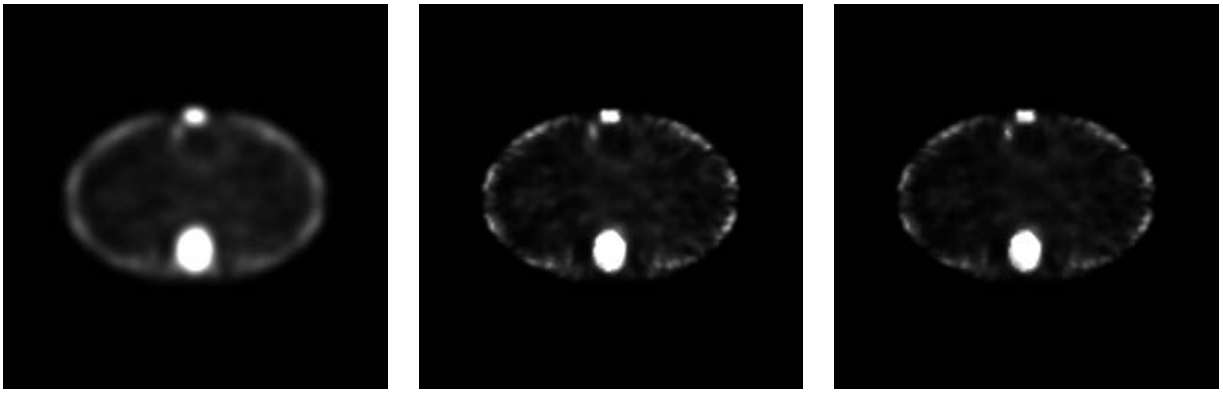

no prior (RBI) | MAP, organ only (sO) | MAP, organ & lesion boundaries (sO+L)

Fig. 1. Anecdotal reconstructions of one simulated case using three strategies. A lesion is visible to the lower left of the sternum. The anatomical priors sharpen the edges of the organs (middle) and organs and lesion (right).

boundaries. The system model included corrections for attenuation, scatter, and 3-D depth-dependent resolution. The same two values of β were used as for the simple quadratic prior.

Table I summarizes the reconstruction strategies. All MAP strategies were computed using the De Pierro algorithm, with an iteration strategy intended to achieve convergence [12]. A sample lesion-present data set reconstructed using three strategies is shown in figure 1.

C. Observer study

Transverse slices were then extracted from the images for analysis by the observers. This resulted in 300 simulated cases, of which exactly half included a lesion. We partitioned these into 100 training images and 200 study images.

The study began by having each observer read the 100 training cases reconstructed by each algorithm (total of 900 training images). After reading an image, the observer clicked the mouse on the most likely lesion location, and indicated how confident he was that a lesion is present at that location.

During training the computer provided feedback about lesion presence and location after each image. After completing initial training, we had each observer read two study sets per algorithm (total of 18 sets). Each study set consisted of 50 retraining images, for which feedback was again provided, followed by 100 study images with no feedback (total of 1800 study images). Each observer read the sets in a different order.

Our observers were three scientists from our medical-physics group, and two nuclear-medicine physicians from our clinic.

III. RESULTS & DISCUSSION

Figure 2 shows the average area under the LROC curve for each algorithm. The bars indicate reader variability for that algorithm, ranging from the lowest area to the highest area. Algorithms sO+L (strong anatomical prior giving both organ and true lesion boundaries) and sO+P (strong anatomical prior giving organ, true lesion, and pseudo-lesion boundaries) had the best performance. The lowest-performing reader using these algorithms beat the highest-performing reader using RBI.

Two-way ANOVA indicates that there is a statistically significant difference in average AUC between the algorithms, and also a statistically significant reader effect ($p < 10^{-8}$). A pairwise comparison using Tukey's Honest Significant Difference (HSD) test shows that the four strategies using prior knowledge about lesion boundaries (wO+L, sO+L, wO+P, sO+P) are all superior to RBI ($p < 0.05$).

However, the two strategies with just organ boundaries (wO, sO) are not significantly better than RBI. This is unfortunate,

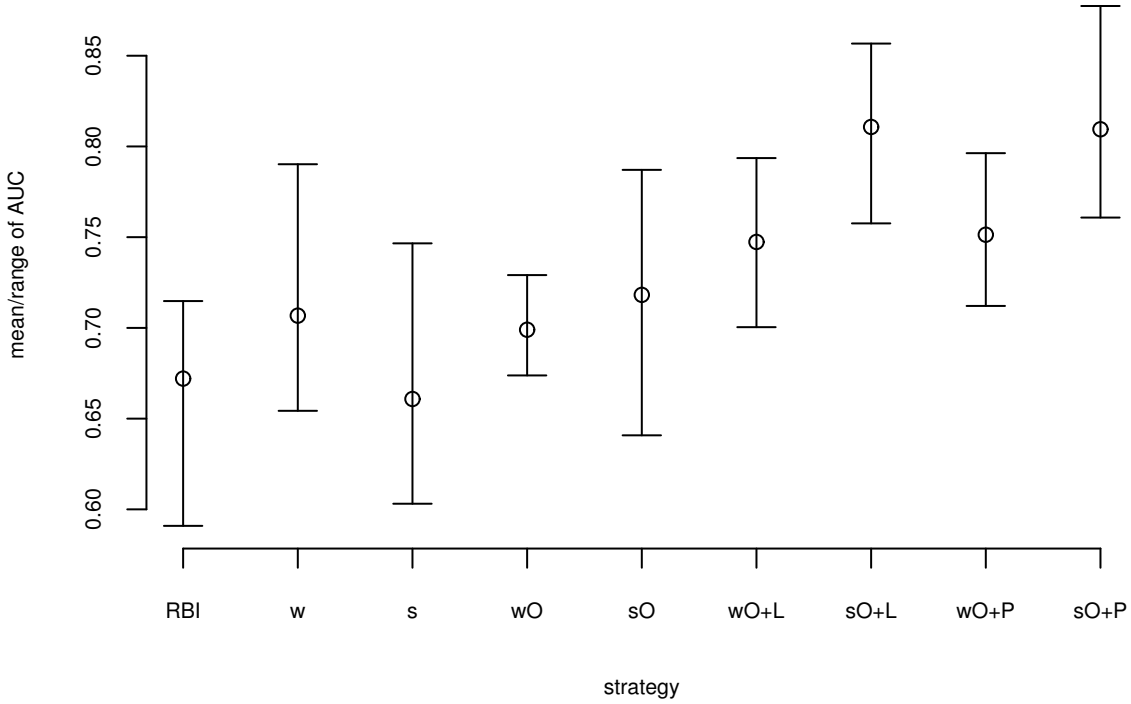

Fig. 2. Average area (5 human observers) under the LROC curve for each reconstruction strategy. The bars indicate reader variability, ranging from the reader with the lowest AUC for that algorithm to the reader with the highest AUC.

as the situation in which a lesion is visible in SPECT but not in CT occurs in clinical practice.

For MAP reconstruction with simple quadratic smoothing, strengthening the prior decreases performance (w vs. s), while for all the anatomical priors strengthening the prior increases performance. Our pilot study with model observers predicted we would not see much change in AUC between these prior strengths. Finding a larger difference than expected suggests that we may not have yet found the best value of β. Thus by optimizing β it may be possible to find an anatomical MAP strategy with even better performance than the strategies shown here.

This study does not address two important issues. The first has to do with how to best provide the observer with the fruits of high-resolution anatomical knowledge. Here we have done so by incorporating anatomy into the SPECT reconstruction process, but have not given the observer direct access to the anatomical data. However in SPECT/CT clinical practice the physician will fuse the SPECT and CT images, which has been shown to help lesion localization [13]. How much does incorporating an anatomical prior into SPECT reconstruction improve observer performance when the observer has direct access to the high-resolution anatomical data?

The second has to do with mismatch between the prior and the SPECT acquisition. For example there might be registration error between the anatomy and the SPECT data, or there might be segmentation errors in the anatomical prior. How accurate does the anatomical model need to be to get a significant improvement in observer performance?

IV. Conclusion

Lesion-detection accuracy improves when prior knowledge of both the organ and the lesion boundaries is incorporated into the SPECT reconstruction process. Including pseudo lesions, regions defined in the prior which do not have increased uptake, does not degrade performance. Prior knowledge of only the organ boundaries, but not the lesion boundaries, does not improve performance by a statistically significant amount. The possibility exists of further improvement in observer performance through optimization of β.

References

[1] P. P. Bruyant, H. C. Gifford, G. Gindi, and M. A. King, "Investigation of observer-performance in MAP-EM reconstruction with anatomical priors and scatter correction for lesion detection in ^{67}Ga images," in *2003 IEEE Nuclear Science Symposium Conference Record*, Oct. 2003, pp. 3166–9, Vol. 5.

[2] ——, "Numerical observer study of MAP-OSEM regularization methods with anatomical priors for lesion detection in ^{67}Ga images," *IEEE Trans. Nucl. Sci.*, vol. 51, no. 1, pp. 193–7, Feb. 2004.

[3] P. P. Bruyant, H. C. Gifford, G. Gindi, P. H. Pretorius, and M. A. King, "Human and numerical observer studies of lesion detection in Ga-67 images obtained with MAP-EM reconstructions and anatomical priors," in *2004 IEEE Nuclear Science Symposium Conference Record*, Oct. 2004, pp. 4072–5, Vol. 7.

[4] S. Kulkarni, P. Khurd, I. Hsiao, and G. Gindi, "Effect on lesion detectability of proximity to anatomical boundaries in emission tomography," in *2005 IEEE Nuclear Science Symposium Conference Record*, Oct. 2005, pp. 2150–4.

[5] S. P. Bartold, K. J. Donohoe, J. W. Fletcher, T. P. Haynie, R. E. Henkin, E. B. Silberstein, H. D. Royal, and A. Van den Abbeele, "Procedure guideline for gallium scintigraphy in the evaluation of malignant disease." *J. Nucl. Med.*, vol. 38, no. 6, pp. 990–4, June 1997.

[6] E. Bombardieri, C. Aktolun, R. P. Baum, A. Bishof-Delaloye, J. Buscombe, J. F. Chatal, L. Maffioli, R. Moncayo, L. Mortelmans, and S. N. Reske, "^{67}Ga scintigraphy: procedure guidelines for tumour imaging," *Eur. J. Nucl. Med. Mol. Imaging*, vol. 30, no. 12, pp. BP125–31, Dec. 2003.

[7] B. M. W. Tsui, X. D. Zhao, G. K. Gregoriou, D. S. Lalush, E. C. Frey, R. E. Johnston, and W. H. McCartney, "Quantitative cardiac SPECT reconstruction with reduced image degradation due to patient anatomy," *IEEE Trans. Nucl. Sci.*, vol. 41, no. 6, pp. 2838–44, Dec. 1994.

[8] P. Pretorius, M. A. King, T.-S. Pan, and B. Hutton, "Attenuation correction strategies for multi-energy photon emitters using SPECT," *IEEE Trans. Nucl. Sci.*, vol. 44, no. 3, pp. 1323–8, June 1997.

[9] M. Ljungberg and S.-E. Strand, "A Monte Carlo program for the simulation of scintillation camera characteristics," *Comput. Methods Programs Biomed.*, vol. 29, no. 4, pp. 257–72, Aug. 1989.

[10] C. L. Byrne, "Accelerating the EMML algorithm and related iterative algorithms by rescaled block-iterative methods," *IEEE Trans. Image Process.*, vol. 7, no. 1, pp. 100–9, Jan. 1998.

[11] H. C. Gifford, M. A. King, M. V. Narayanan, P. H. Pretorius, and M. S. Smyczynski, "Effect of block-iterative acceleration of Ga-67 tumor detection in thoracic SPECT," *IEEE Trans. Nucl. Sci.*, vol. 49, no. 1, pp. 50–5, Feb. 2002.

[12] A. R. De Pierro, "A modified expectation maximization algorithm for penalized likelihood estimation in emission tomography," *IEEE Trans. Med. Imag.*, vol. 14, no. 1, pp. 132–7, Mar. 1995.

[13] B. Palumbo, S. Sivolella, I. Palumbo, A. M. Liberati, and R. Palumbo, "^{67}Ga-SPECT/CT with a hybrid system in the clinical management of lymphoma," *Eur. J. Nucl. Med. Mol. Imaging*, vol. 32, no. 9, pp. 1011–7, Nov. 2005.